Analysis of Spacecraft Motion Under Constant Circumferential Propulsive Acceleration

Alessandro A. Quarta *, Giovanni Mengali

Department of Civil and Industrial Engineering, University of Pisa,

I-56122 Pisa, Italy

This paper is dedicated to the memory of Dr. Richard H. Battin.

Abstract

This paper reassesses the classical circumferential-thrust problem, in which a spacecraft orbiting around a primary body is subjected to a propulsive acceleration of constant modulus, whose direction is in the plane of the parking orbit and orthogonal to the spacecraft-primary line. In particular, a new formulation is proposed to obtain a reduction in the number of differential equations required for the study of the spacecraft propelled trajectory. The mathematical complexity of the problem may be further reduced assuming that both the propulsive acceleration modulus and the spacecraft distance from the primary body are sufficiently small. In that case, an approximate model is able to accurately describe the characteristics of the propelled trajectory when the parking orbit is circular. Finally, using the data obtained by numerical simulations, the approximate model is extended to generate a set of semi-analytical equations for the analysis of a classical escape mission scenario.

Key words: Circumferential Thrust, Escape Trajectories, Low-Thrust Mission Analysis

Nomenclature

$\boldsymbol{a}_p$	=	propulsive acceleration, with $a_p \triangleq \|\boldsymbol{a}_p\|$
$\mathcal{E}$	=	specific mechanical energy
h	=	angular momentum modulus
n	=	best-fit parameter
O	=	primary body's center-of-mass
p	=	osculating orbit's semilatus rectum
r	=	primary-spacecraft distance
t	=	time
$\mathcal{T}$	=	polar reference frame
u	=	radial component of the spacecraft velocity
v	=	circumferential component of the spacecraft velocity
y	=	auxiliary variable, see Eq. (9)
ϵ	=	tolerance
μ	=	gravitational parameter
τ	=	thrusting parameter
θ	=	polar angle

Subscripts

0	=	initial, parking orbit
esc	=	escape

* Corresponding author.
Email addresses: a.quarta@ing.unipi.it (Alessandro A. Quarta),
g.mengali@ing.unipi.it (Giovanni Mengali).

max	=	maximum
m	=	reference value

Superscripts

$\sim$	=	dimensionless
$'$	=	derivate w.r.t. p
$\cdot$	=	time-derivative

1 Introduction

A considerable interest still exists for analytical, albeit approximate, solutions to spaceflight mechanics problems in which a spacecraft is equipped with a thruster that provides a continuous, low-thrust acceleration. The main reason, besides the importance of obtaining an accurate physical description of the spacecraft motion, lies in its usefulness in the preliminary design of orbit transfers and in its importance in providing initial guesses for trajectory optimization purposes [1,2,3]. A significant example is given by the tangential thrust problem [4,5], where the direction of the propulsive acceleration vector is aligned with the direction of the spacecraft (orbital) velocity vector.

A special class of spaceflight mechanics problems, within which an analytical solution has been sought, involves a spacecraft subjected to a propulsive acceleration with a constant modulus, and a fixed direction in an orbital reference frame. A classical problem of this kind is the radial-thrust problem [6,7,8,9], in which the propulsive acceleration direction coincides with the spacecraft-primary line. In that case, an analytical approach to the trajectory determination problem is partially simplified by the existence of a constant of motion, namely the specific angular momentum. Its "companion" problem, according to the classical work of Tsien [6], is the case of circumferential-thrust and is the subject of this paper. In that scenario, the spacecraft is subjected to a propulsive acceleration (of constant modulus) whose direction is orthogonal, at any time, to the direction of the local gravity due to the primary body.

An interesting result for the circumferential-thrust problem, when the parking orbit is circular, is summarized in Battin's textbook [10]. In his simplified analysis, Battin postulates that for sufficiently small values of circumferential propulsive acceleration modulus, the radial (net) acceleration may be neglected, so that the centripetal acceleration is approximately balanced by the gravity from the primary body. As a consequence of such an assumption, some analytical (approximate) relationships involving the escape distance, the time required to attain an escape condition and the number of revolutions about the primary body can be obtained [10].

The aim of this paper is to reassess the circumferential-thrust problem from a different viewpoint. Firstly, it is shown how the original differential problem may be reduced to a simpler system with the aid of a suitable change of variable. The new formulation is the starting point for introducing a different simplification criterion. In fact, unlike what is pointed out in Ref. [10], it will be shown that a small value of propulsive acceleration modulus is not, in itself, a condition sufficient to guarantee accurate results, but it is required instead that the product between the propulsive acceleration modulus and the spacecraft-primary distance be sufficiently small. Under such a new assumption, it is possible to obtain more accurate analytical relationships, which approximate the spacecraft state along the propelled trajectory. Finally, using the data obtained from numerical simulations, the approximate model is used to generate a set of semi-analytical relationships that are useful for estimating the spacecraft state when it reaches the escape condition from the primary body.

2 Equations of motion

Consider a spacecraft that initially tracks a circular parking orbit, of radius r_0, around a primary body of gravitational parameter μ. Starting from the reference time $t = t_0 \triangleq 0$ the propulsion system provides a circumferential thrust in the plane of the parking orbit, that is, a thrust whose direction is normal to the spacecraft-primary line. The corresponding propulsive acceleration vector $\boldsymbol{a}_p$ is assumed both to be of constant modulus, and to belong to the parking orbit plane. Accordingly, the spacecraft motion can be described by means of a polar reference frame $\mathcal{T}(O; r, \theta)$, where the origin coincides with the center-of-mass O of the primary body, see Fig. 1. Note that the polar angle θ is measured counterclockwise from the direction of the spacecraft position vector at the reference time t_0. In that scenario, the spacecraft equations of motion are:

$$\dot{r} = u \tag{1}$$

$$\dot{\theta} = \frac{v}{r} \tag{2}$$

$$\dot{u} = -\frac{\mu}{r^2} + \frac{v^2}{r} \tag{3}$$

$$\dot{v} = -\frac{u\,v}{r} + \tau\, a_p \tag{4}$$

where r is the primary body-spacecraft distance, u and v are, respectively, the radial and circumferential components of the spacecraft velocity, and $a_p \triangleq \|\boldsymbol{a}_p\|$ is the (constant) modulus of the propulsive acceleration vector. In Eq. (4), the term $\tau \in \{-1, 1\}$ is a dimensionless parameter that models the direction of the propulsive acceleration vector, which may be used to either increase ($\tau = 1$) or to decrease ($\tau = -1$) the specific angular momentum $h \triangleq r\,v$ of the osculating orbit.

Note that the mathematical model discussed in this paper does not include the case of $\tau = 0$, thus avoiding the existence of coasting arcs along the spacecraft (propelled) trajectory.

2.1 Reduction of the differential system

The differential system of Eqs. (1)–(4) may be reduced to a simpler system of three differential equations with the aid of a suitable change of variable. To this end, it is convenient to introduce the semilatus rectum of the osculating orbit, $p \triangleq h^2/\mu$. Bearing in mind Eqs. (1) and (4), and observing that $\dot{h} = \dot{r}v + r\dot{v}$, the time-derivative of the semilatus rectum is

$$\dot{p} = \frac{2\,r\,\tau\,a_p\,h}{\mu} \tag{5}$$

From the last equation, the first and second time-derivative of the distance r and the first time-derivative of the polar angle θ can be written as:

$$\dot{r} = \frac{\tau\, a_p\, h}{\mu}\, \frac{\mathrm{d}(r^2)}{\mathrm{d}p} \tag{6}$$

$$\ddot{r} = \frac{r\, \left(\tau\, a_p\right)^2}{\mu} \left[\frac{\mathrm{d}(r^2)}{\mathrm{d}p} + 2\, p\, \frac{\mathrm{d}^2(r^2)}{\mathrm{d}p^2}\right] \tag{7}$$

$$\dot{\theta} = \frac{2\, r\, \tau\, a_p\, h}{\mu}\, \frac{\mathrm{d}\theta}{\mathrm{d}p} \tag{8}$$

Introduce now the following dimensionless quantities

$$\widetilde{r} \triangleq \frac{r}{r_0} \quad , \quad y \triangleq \widetilde{r}^2 \quad , \quad \widetilde{a}_p \triangleq \frac{a_p}{(\mu/r_0^2)} \quad , \quad \widetilde{p} \triangleq \frac{p}{r_0} \tag{9}$$

Since the parking orbit is circular, it follows that $p(t_0) = r_0$, from which $\widetilde{p}(t_0) = 1$. The dimensionless equations of motion are obtained from Eqs. (6)–(8) using $\widetilde{p}$ as the independent variable, viz.

$$\theta' = \frac{1}{2\, \tau\, \widetilde{a}_p\, \sqrt{y^3}} \tag{10}$$

$$y'' = -\frac{1}{2\, \widetilde{p}} \left[y' + \frac{\sqrt{y} - \widetilde{p}}{\left(\tau\, \widetilde{a}_p\, y\right)^2}\right] \tag{11}$$

where the prime symbol represents a derivative taken with respect to $\widetilde{p}$. Note that the previous assumption of $\tau \neq 0$ (namely the exclusion of coasting arcs along the spacecraft trajectory) avoids any singularity in the denominator of Eq. (11).

The two differential equations (10)-(11) are completed by the following three initial conditions calculated at $t = t_0$, when $\widetilde{p} = 1$:

$$\theta|_{\widetilde{p}=1} = 0 \quad , \quad y|_{\widetilde{p}=1} = 1 \quad , \quad y'|_{\widetilde{p}=1} = 0 \tag{12}$$

where the last initial condition comes from the fact that $\dot{r}(t_0) = 0$ implies

$\mathrm{d}(r^2)/\mathrm{d}p(t_0) = 0$, see Eq. (6).

Note that Eqs. (10)-(11) do apply to an elliptic parking orbit as well. In that case r_0 is the initial spacecraft distance from the primary body and the first two initial conditions in Eqs. (12) remain unchanged. The condition involving y', instead, must be changed to take into account the actual spacecraft radial velocity at the starting point, see Eq. (6).

Returning to the differential system (10)-(11), it is apparent that the equation in y is independent of θ. Also, the first order differential equation in θ can be integrated numerically when a solution $y = y(\widetilde{p})$ has been found. However, the second order differential equation (11) seems to admit of no analytical solution, even if an approximate relationship $y = y(\widetilde{p})$ may be obtained using some additional assumption, as will be discussed now.

2.2 Analytical Approximation

Equation (11) can be rearranged to obtain a simplified relationship in the form $y = y(\widetilde{p})$. To that end, note that the equivalent form of Eq. (11) is

$$(2\,\widetilde{p}\,y'' + y')\,(\tau\,\widetilde{a}_p\,y)^2 = \widetilde{p} - \sqrt{y} \tag{13}$$

Under the assumption $\widetilde{a}_p\,y \ll 1$, it is found that

$$\sqrt{y} \simeq \widetilde{p} \tag{14}$$

In other terms, taking into account the definition of y from Eq. (9), when the product $\widetilde{a}_p\,y$ is sufficiently small the semilatus rectum of the osculating orbit is approximately equal to the distance r of the spacecraft from the center-of-mass O. This is in accordance with results of Ref. [10] even if the latter was obtained using a conceptually different approach. In fact, the analysis described in Ref. [10] postulates that when the modulus of the propulsive acceleration is sufficiently small (or, using the notation of this paper, when $\widetilde{a}_p \ll 1$), the centripetal acceleration (v^2/r) is approximately balanced by the gravity pull (μ/r^2) in such a way that the radial acceleration is nearly zero ($\dot{u} \simeq 0$). Therefore, according to Ref. [10], the spacecraft trajectory is well approximated by a spiral curve with a small flight path angle and the circumferential velocity v is, in fact, nearly equal to the local circular velocity $\sqrt{\mu/r}$. This implies that the semilatus rectum of the osculating orbit is close to r, i.e. the eccentricity of the osculating orbit is very small.

Actually, Eq. (13) shows that a small value of propulsive acceleration is not sufficient to guarantee that $p \simeq r$, but it is required that $\widetilde{a}_p\, y$ be sufficiently small. This in its turn implies that y should not increase too much with time. However, the latter assumption may not be sound in some mission scenarios. Consider, for example, a case in which $\tau = 1$, that is, a trajectory in which the angular momentum (and so the spacecraft distance from point O) tends to increase with time. It is clear that the assumption $p \simeq r$ will become more and more approximate over time as long as the spacecraft moves away from the parking orbit.

This behaviour is highlighted in Fig. 2, which is the result of the numerical integration of Eq. (11) taking into account the boundary conditions of Eqs. (12). Figure 2 shows the variation of the dimensionless distance $\widetilde{r}$ when $\widetilde{a}_p = 0.5\%$ and $\tau = 1$. During the first phase of motion, roughly as long as $\widetilde{r} < 5$, the approximation of Eq. (14) is reasonable because the difference between $\widetilde{r}$ and $\widetilde{p}$ is less than 5%. As $\widetilde{r}$ increases, the difference between $\widetilde{r}$ and $\widetilde{p}$ becomes larger and larger and the approximation of Eq.(14) loses its accuracy. Nevertheless, Eq. (14) is a good starting point for the development of a semi-analytical model to estimate the characteristics of the spacecraft (propelled) trajectory also when the product $\widetilde{a}_p\, y$ is not sufficiently small, as in the case of the attainment of the escape conditions from the primary body.

Under the assumption $\widetilde{a}_p\, y \ll 1$, there exists a maximum dimensionless distance $\widetilde{r}_m \triangleq \sqrt{y_m}$ within which the approximation of Eq. (14) is reasonable when $\tau = 1$. A possible way to calculate such a (critical) distance is as follows. For a given value of $\widetilde{a}_p$, the differential equation (11) may be numerically integrated. The value y_m is the value of the numerically calculated y such that the condition

$$\left| \frac{\sqrt{y_m}}{\widetilde{p}} - 1 \right| = \epsilon \tag{15}$$

is met, where ϵ is a sufficiently small (and given) value. The variation of $\widetilde{r}_m$ with both the propulsive acceleration modulus $\widetilde{a}_p \in [0.1\%, 1\%]$ and the parameter ϵ can be found numerically once and for all. The simulation results have been obtained using a variable order Adams-Bashforth-Moulton solver scheme [11], with absolute and relative errors of 10^{-12}, and the results are summarized in Fig. 3.

For example, when $\widetilde{a}_p = 0.5\%$ and $\epsilon = 5\%$, Fig. 3 states that $\widetilde{r}_m \simeq 5$. This means that the difference between the numerical solution of Eq. (13) and the approximate value given by Eq. (14) is less than 5% as long as the spacecraft distance from point O is less than about five times the radius r_0 of the (circular) parking orbit. This result is, as expected, in accordance with Fig. 2. The simulations also show that for inner trajectories (that is, when $\tau = -1$), the approximation of Eq. (14) provides a result close to the numerical solution provided that $\widetilde{a}_p < 0.01$. Indeed, in this scenario, both the distance r and the product $\widetilde{a}_p\, y$ decrease with time.

It is worth noting that the condition $\sqrt{y} \simeq \widetilde{p}$, within the previously discussed limits of effectiveness, allows one to obtain an approximate expression for the spacecraft trajectory and for the radial (u) and circumferential (v) velocities. Indeed, combining Eq. (14) with Eq. (6), the result is

$$\widetilde{u} \triangleq \frac{u}{\sqrt{\mu/r_0}} \simeq 2\,\tau\,\widetilde{a}_p\,\sqrt{\widetilde{p}^3} \quad , \quad \widetilde{v} \triangleq \frac{v}{\sqrt{\mu/r_0}} \simeq 1/\sqrt{\widetilde{p}} \tag{16}$$

Also, substituting Eq. (14) into Eq. (10) and integrating after a variable separation, it is found that

$$\widetilde{r} \simeq \frac{1}{\sqrt{1 - 4\,\tau\,\widetilde{a}_p\,\theta}} \tag{17}$$

where the polar angle θ is zero at the beginning of the propelled phase, see Fig. 1. From the last equation the maximum value of angle swept out by the spacecraft during the propelled phase is $\theta_{\max} \triangleq 1/(4\,\widetilde{a}_p)$, because Eq. (17) states that when $\theta \to \theta_{\max}$, the distance from the primary body tends to infinity.

A closed (approximate) form of the spacecraft distance r as a function of time t can be obtained using Eq. (14). This is possible by integrating the first of Eqs. (16) after a variable separation, and the result coincides, as expected, with the dimensionless form of the relationship discussed in Ref. [10], viz.

$$\widetilde{r} \simeq \frac{1}{\left(1 - \tau\,\widetilde{a}_p\,\widetilde{t}\right)^2} \tag{18}$$

where $\widetilde{t} \triangleq t/\sqrt{r_0^3/\mu}$ is, in fact, the dimensionless time.

3 Analysis of the Escape Conditions

The achievement of escape conditions for a spacecraft equipped with a low-thrust propulsion system is a classical mission scenario, which, of course, has been studied even under the assumption of a circumferential-thrust strategy [6,10]. The aim of this section is to investigate whether the previous analytical model may be useful for approximating the escape conditions of the spacecraft. Starting from Eq. (14), the problem reduces to estimating the distance, the spacecraft velocity components and the number of revolutions around the primary when the mechanical energy of the osculating orbit goes to zero.

From the definition of h and the expression of u given by Eq. (6) the specific mechanical energy of the osculating orbit $\mathcal{E} \triangleq (u^2 + v^2)/2 - \mu/r$ can be written as a function of both the dimensionless semilatus rectum p and the auxiliary variable y, viz.

$$\widetilde{\mathcal{E}} \triangleq \frac{\mathcal{E}}{\mu/(2\, r_0)} = \widetilde{p}\, \left(\tau\, \widetilde{a}_p\, y'\right)^2 + \frac{\widetilde{p}}{y} - \frac{2}{\sqrt{y}} \tag{19}$$

Note that $\mu/(2\, r_0)$ is the modulus of the specific mechanical energy along the (circular) parking orbit.

Using the approximation of Eq. (14) and taking into account that $\tau^2 = 1$, Eq. (19) provides an expression for the dimensionless specific mechanical energy of the osculating orbit as a function of the dimensionless propulsive acceleration modulus and the distance from the primary body only:

$$\widetilde{\mathcal{E}} \simeq 4\, \widetilde{r}^3\, \widetilde{a}_p^2 - \frac{1}{\widetilde{r}} \tag{20}$$

It is worth noting that Eq. (20) is consistent with the initial conditions (i.e. $\widetilde{\mathcal{E}} = -1$ when $\widetilde{r} = 1$) only if the propulsive acceleration modulus is zero. In fact, this represents the limiting case in which the spacecraft keeps its initial orbit and, as such, it does not vary its specific mechanical energy.

According to Ref. [10], from Eqs. (14) and (20) the dimensionless distance

$\widetilde{r}$ at which the escape condition $\widetilde{\mathcal{E}} = 0$ is met is

$$\widetilde{r}|_{\widetilde{\mathcal{E}}=0} \triangleq \widetilde{r}_{\rm esc} \simeq \frac{1}{\sqrt{2\,\widetilde{a}_p}} \tag{21}$$

whereas the corresponding polar angle is obtained by combining Eq. (21) with (17), viz.

$$\theta|_{\widetilde{\mathcal{E}}=0} \triangleq \theta_{\rm esc} \simeq \frac{1}{4\,\widetilde{a}_p} - \frac{1}{2} \tag{22}$$

Finally, the components of spacecraft velocity at the escape are found by substituting Eq. (21) into Eq. (16) and taking into account the approximation of Eq. (14):

$$\widetilde{u}|_{\widetilde{\mathcal{E}}=0} \triangleq \widetilde{u}_{\rm esc} \simeq \sqrt[4]{2\,\widetilde{a}_p} \quad , \quad \widetilde{v}|_{\widetilde{\mathcal{E}}=0} \triangleq \widetilde{v}_{\rm esc} \simeq \sqrt[4]{2\,\widetilde{a}_p} \tag{23}$$

The approximate analytical relationships (21)–(23), which fully describe the state of the spacecraft when $\widetilde{a}_p\, y \ll 1$ and the escape condition ($\widetilde{\mathcal{E}} = 0$) is met, point out that the generic state variable scales with the dimensionless propulsive acceleration as $\widetilde{a}_p^n$, where n is a suitable exponent (for example $n = -1/2$ for the distance r, see Eq. (21)). Note that according to Eq. (23) the two velocity components (u and v) take the same value at the escape condition. This would imply a flight path angle of 45 deg when $\widetilde{\mathcal{E}} = 0$, which is well beyond the typical value of a few degrees that characterizes a (nearly-spiral) trajectory in which the approximation of Eq. (14) is sound [10]. Indeed, Eq. (21) clearly states that $\widetilde{r}_{\rm esc}^2\, \widetilde{a}_p \equiv y_{\rm esc}^2\, \widetilde{a}_p \simeq 1/2$, and therefore the assumption behind the analytical approximation (i.e. $\widetilde{a}_p\, y \ll 1$) is grossly violated near escape. Accordingly, it is possible that the analytical results given by Eqs. (21)–(23) may not be able to model the state of the spacecraft in an effective way.

To better investigate this problem the state of the spacecraft at the escape has been calculated by integrating numerically Eq. (11), in which the dimensionless propulsive acceleration is varied within the interval $\widetilde{a}_p \in [0.01\%, 5\%]$. The aim of this analysis is also to check the existence of a possible correlation between the components of the state vector of the spacecraft at the escape (that is, $\widetilde{r}_{\rm esc}$, $\theta_{\rm esc}$, $\widetilde{u}_{\rm esc}$, and $\widetilde{v}_{\rm esc}$) and the dimensionless propulsive acceleration $\widetilde{a}_p$. The results have been arranged in a graphical form, where the circles represent the outputs from the numerical integration, while the dashed line describes what is obtained from the approximate relationships. For example, Fig. 4 shows the variation of the (escape) polar angle $\theta_{\rm esc}$ as a function of $1/\widetilde{a}_p$. In this case the approximate relationship, given by Eq. (22), is able to capture very well the actual value of $\theta_{\rm esc}$.

The situation is much different when the escape distance $\widetilde{r}_{\rm esc}$ is considered, see Fig. 5. The numerical results show that $\widetilde{r}_{\rm esc}$ varies nearly linearly with $1/\sqrt{\widetilde{a}_p}$, but the results provided by Eq. (21) are inaccurate.

Nevertheless, the topology of the curve in Fig. 5 suggests that a more accurate estimate of the escape distance can be obtained by refining the analytical approximation using the results from the numerical integration. In fact, a much better approximation of the value of $\widetilde{r}_{\rm esc}$ can be obtained by interpolating the numerical results with a polynomial function in the variable $1/\sqrt{\widetilde{a}_p}$. Using a first order polynomial, the escape distance can be approximated with an error less than 5% (assuming $\widetilde{a}_p < 1\%$) through the function

$$\widetilde{r}_{\rm esc} \simeq \frac{0.8527}{\sqrt{\widetilde{a}_p}} \tag{24}$$

Likewise, a correlation between the approximation of Eq. (23) and the corresponding numerical results also exists for the two velocity components $\widetilde{u}_{\rm esc}$ and $\widetilde{v}_{\rm esc}$, as is shown in Fig. 6. In particular, the analytical model tends to overestimate $\widetilde{u}_{\text{esc}}$, while the value of $\widetilde{v}_{\text{esc}}$ is slightly underestimated. Nevertheless, Fig. 6 clearly shows that both $\widetilde{u}_{\text{esc}}$ and $\widetilde{v}_{\text{esc}}$ vary linearly with $\sqrt[4]{\widetilde{a}_p}$ (especially for small values of the propulsive acceleration modulus), in analogy with what suggested by Eq. (23). It is therefore reasonable to use a first order polynomial to obtain a best fit approximation of the numerical result, and the following functions are found

$$\widetilde{u}_{\text{esc}} \simeq 0.8187 \sqrt[4]{\widetilde{a}_p} \qquad , \qquad \widetilde{v}_{\text{esc}} \simeq 1.294 \sqrt[4]{\widetilde{a}_p} \tag{25}$$

It can be verified that the previous formulas approximate the numerical values with a maximum error less than 0.15% only, assuming a dimensionless propulsive acceleration modulus $\widetilde{a}_p \leq 1\%$.

To summarize, the semi-analytical relationships (22), (24), and (25) provide an accurate approximation of the spacecraft state when an escape condition is attained. In particular, assuming $\widetilde{a}_p < 1\%$, the polar angle θ_{esc} and the two velocity components $\widetilde{u}_{\text{esc}}$ and $\widetilde{v}_{\text{esc}}$ are estimated with maximum percentage errors less than 0.15%, while the error in the escape distance $\widetilde{r}_{\text{esc}}$ does not exceed the 5% limit.

4 Conclusions

The classical problem of a two-dimensional motion of a spacecraft subjected to a constant, circumferential, propulsive acceleration has been revisited. Two main contributions have been discussed in the paper. Firstly, a new and exact analytical approach has been proposed in order to reduce the number of differential equations of the problem and to simplify its numerical solution.

In particular, under the assumption that the product between the propulsive acceleration (dimensionless) modulus and the spacecraft-primary body (dimensionless) distance is sufficiently small, it is possible to obtain fundamental informations about the spacecraft state as, for example, its velocity components and the characteristics of the osculating orbit at a given distance from the primary body. In the second place, using the results from the numerical simulations, the approximate model has been extended to provide semi-analytical approximations of the spacecraft state when the escape condition is met.

The complexity reduction of the differential system discussed in this paper can be extended to the more general case of elliptic parking orbit. In that case, however, it is not yet solved the problem of finding a simple and effective relationship that captures the characteristics of the osculating orbit (for example, the value of its semilatus rectum or its eccentricity) as a function of the spacecraft distance from the primary body.

References

[1] A. E. Petropoulos, J. A. Sims, A review of some exact solutions to the planar equations of motion of a thrusting spacecraft, in: 2nd International Symposium on Low-Thrust Trajectory (LoTus-2), Toulouse, France, 2002.

[2] J. T. Betts, Very low-thrust trajectory optimization using a direct SQP method, Journal of Computational and Applied Mathematics 120 (1) (2000) 27–40, doi: 10.1016/S0377-0427(00)00301-0.

[3] D. Izzo, Lambert's problem for exponential sinusoids, Journal of Guidance, Control and Dynamics 29 (5) (2006) 1242–1245, doi: 10.2514/1.21796.

[4] C. Bombardelli, G. Baù, J. Peláez, Asymptotic solution for the two-body problem with constant tangential thrust acceleration, Celestial Mechanics and Dynamical

Astronomy 110 (3) (2011) 239–256, doi: 10.1007/s10569-011-9353-3.

[5] A. E. Petropoulos, Some Analytic Integrals of the Averaged Variational Equations for a Thrusting Spacecraft, Interplanetary Network Progress Report 42-150 (2002) 1–29.

[6] H. S. Tsien, Take-off from satellite orbit, Journal of the American Rocket Society 23 (4) (1953) 233–236 .

[7] F. W. Boltz, Orbital motion under continuous radial thrust, Journal of Guidance, Control, and Dynamics 14 (3) (1991) 667–670, doi: 10.2514/3.20690.

[8] J. E. Prussing, V. L. Coverstone, Constant radial thrust acceleration redux, Journal of Guidance, Control, and Dynamics 21 (3) (1998) 516–518, doi: 10.2514/2.7609.

[9] A. A. Quarta, G. Mengali, New look to the constant radial acceleration problem, Journal of Guidance, Control, and Dynamics 35 (3) (2012) 919–929, doi: 10.2514/1.54837.

[10] R. H. Battin, An Introduction to the Mathematics and Methods of Astrodynamics, AIAA, New York, 1987, p. 418, ISBN: 1-563-47342-9.

[11] L. F. Shampine, M. W. Reichelt, The MATLAB ODE suite, SIAM Journal on Scientific Computing 18 (1) (1997) 1–22, doi: 10.1137/S1064827594276424.

List of Figures

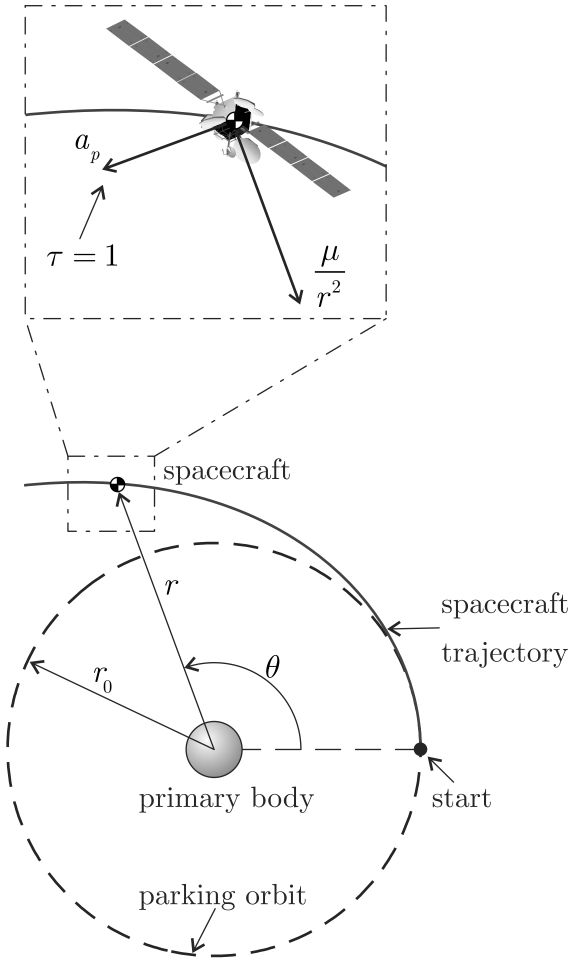

Figure 1. Reference frame.

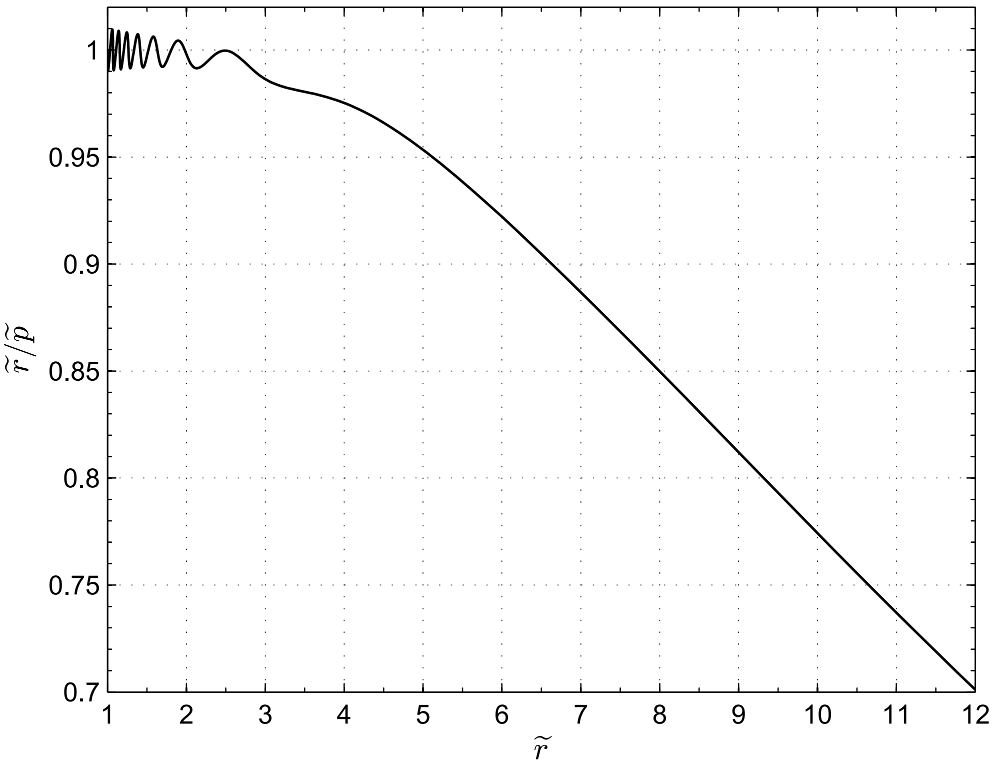

Figure 2. Numerical integration of Eq. (11) when $\widetilde{a}_p = 0.5\%$.

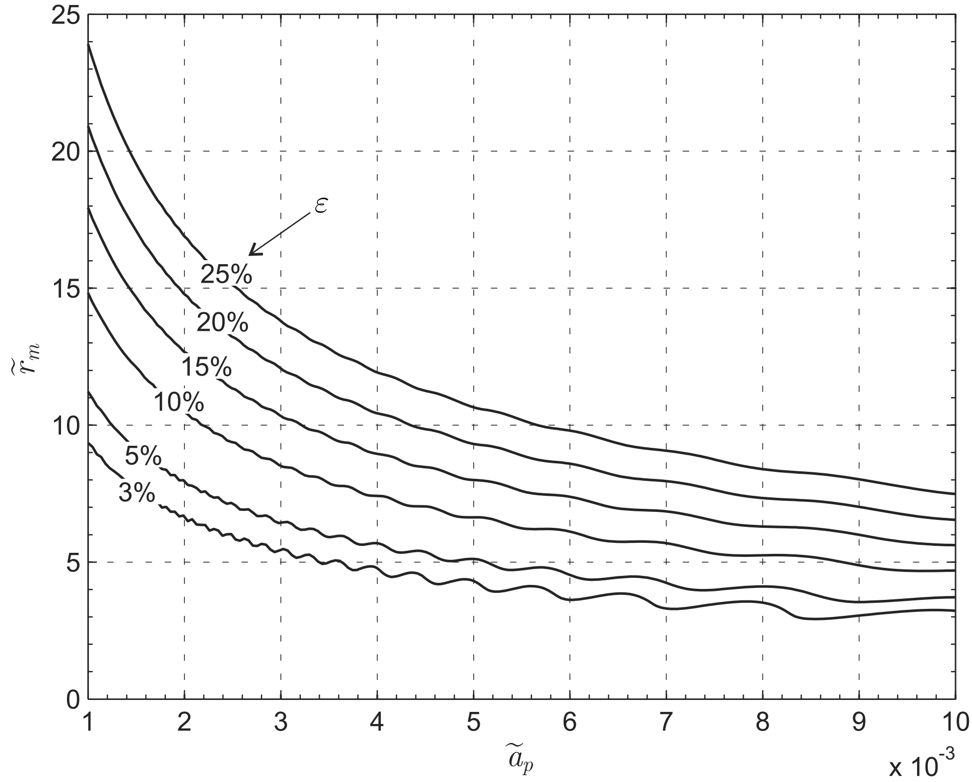

Figure 3. Isocontour of the function $\widetilde{r}_m = \widetilde{r}_m\,(\widetilde{a}_p,\,\epsilon)$.

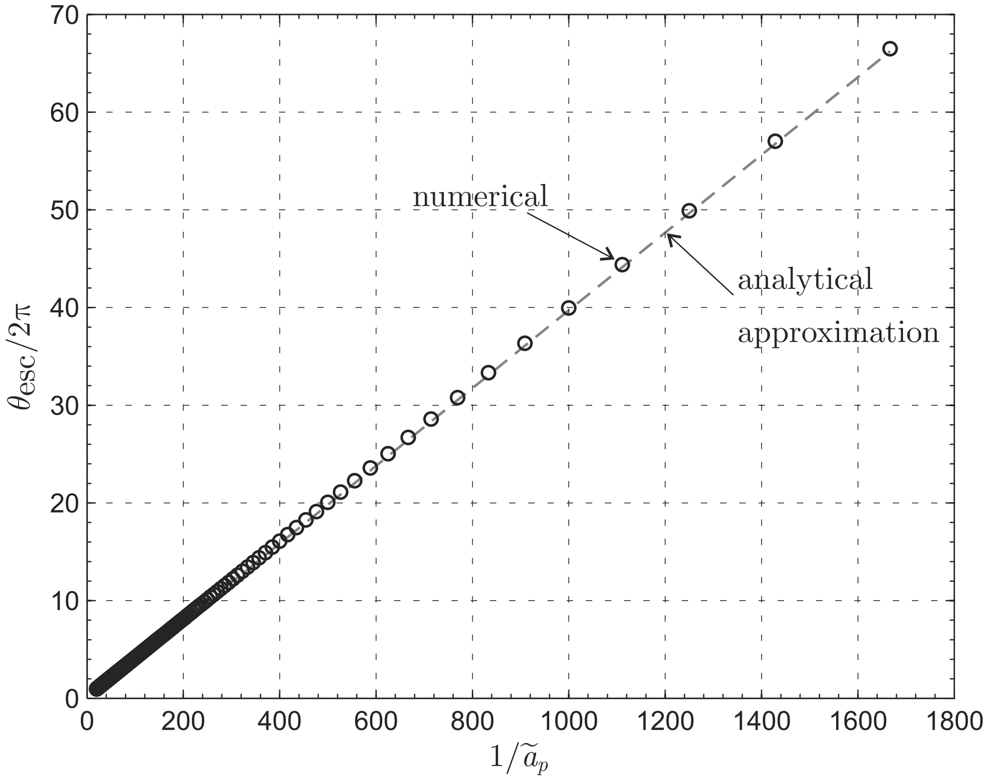

Figure 4. Escape polar angle $\theta_{\rm esc}$ as a function of $\widetilde{a}_p$.

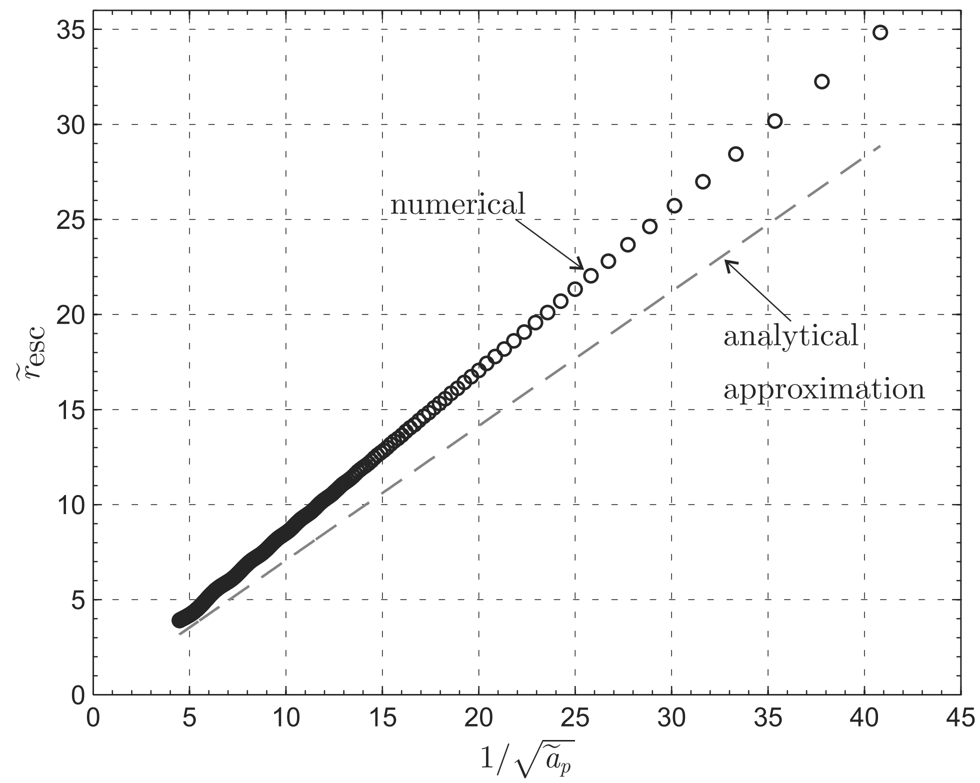

Figure 5. Escape dimensionless radius $\widetilde{r}_{\mathrm{esc}}$ as a function of $\widetilde{a}_p$.

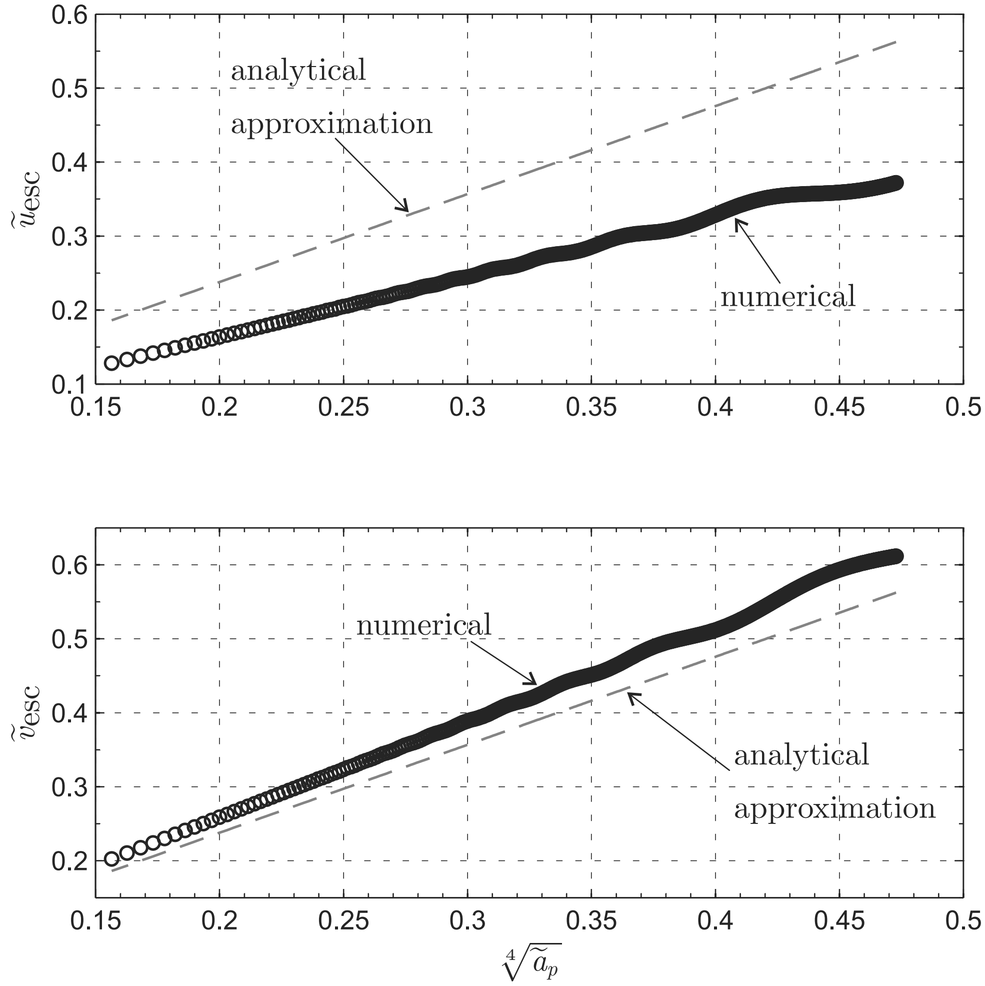

Figure 6. Components of spacecraft dimensionless velocity at the escape, as a function of $\widetilde{a}_p$.